

# Brain Regional Pharmacokinetics of *p*-Aminosalicylic Acid and Its *N*-Acetylated Metabolite: Effectiveness in Chelating Brain Manganese

Lan Hong, Wendy Jiang, Hao Pan, Yueming Jiang, Su Zeng, and Wei Zheng

School of Health Sciences, Purdue University, West Lafayette, Indiana (L.H., W.J., W.Z.); College of Pharmaceutical Sciences, Zhejiang University, Hangzhou, China (L.H., H.P., S.Z.); and Department of Occupational Health and Toxicology, Guangxi Medical University, Nanning, People's Republic of China (Y.J.)

Received May 26, 2011; accepted July 18, 2011

## ABSTRACT:

*para*-Aminosalicylic acid (PAS; 4-amino-2-hydroxybenzoic acid), an antituberculosis drug in use since the 1950s, has recently been suggested to be an effective agent for treatment of manganese-induced parkinsonian disorders. However, the neuropharmacokinetics of PAS and its metabolite *N*-acetyl-*para*-aminosalicylic acid (AcPAS; *N*-acetyl-4-amino-2-hydroxybenzoic acid) are unknown. This study was designed to investigate the pharmacokinetics of PAS and its distribution in brain to help better design the dosing regimen for clinical trials. Male Sprague-Dawley rats received single femoral artery injections of PAS (200 mg/kg). Plasma, cerebrospinal fluid, and brain tissues were collected, and PAS and AcPAS concentrations were quantified by high-performance liquid chro-

matography. After administration, the concentrations of PAS declined rapidly in plasma with an elimination  $t_{1/2}$  of 34 min; the metabolite AcPAS was detected in plasma and eliminated with a  $t_{1/2}$  of 147 min. PAS and AcPAS were detected in brain tissues; AcPAS had a much higher tissue concentration and a longer  $t_{1/2}$  than the parent PAS in most tissues examined. Although both were present in blood or tissues as free, unbound molecules, AcPAS appeared to have a higher tissue affinity than PAS. Taken together, our results suggest that a dosing regimen with continuous intravenous infusion of PAS is necessary to achieve therapeutic levels in targeted brain regions. Furthermore, PAS and AcPAS seem to be effective in reducing manganese levels in brain.

## Introduction

Manganism is mainly due to occupational exposure to manganese (Myers et al., 2003; Crossgrove and Zheng 2004; Bowler et al., 2006; Aschner et al., 2007). Currently, effective clinical treatment options are limited (Cook et al., 1974; Calne et al., 1994; Seaton et al., 1999; Ono et al., 2002). Para-aminosalicylic acid [PAS, 4-amino-2-hydroxybenzoic acid (Paser); CAS number, 65-49-6] has been well known as an antituberculosis drug since the 1950s (Mitnick et al., 2003). The unique structure of PAS, which contains carboxyl and hydroxyl groups, provides the chelating moieties that are essential for manganese binding. Successful treatment of severe chronic manganism with PAS was first reported in two cases of severe manganese poisoning (Ky et al., 1992). A 17-year follow-up study with one of the original patients suggests that PAS therapy needs a long-lasting treatment (Jiang et al., 2006). Additional clinical cases, reported mainly in

Chinese literature, came to similar conclusions (Wu, 1991; Zhao, 1995; Shi, 2002).

The promising therapeutic effect of PAS in the treatment of manganism notwithstanding, its mechanism of action is unclear. Some reports have suggested that the effectiveness of PAS in alleviating parkinsonian syndromes is due to its chelating abilities (Zheng et al., 2009). Other studies have showed that PAS may suppress manganese-induced SK-N-MC cell death because of its anti-inflammatory mechanism (Yoon et al., 2009). A recent study revealed that PAS and EDTA can block manganese toxicity associated with the dopaminergic system; however, the anti-inflammatory agent acetylsalicylic acid does not exhibit a similar effect, leading to the conclusion that the detoxification mechanism of PAS in alleviating Parkinsonism is due primarily to chelation rather than anti-inflammation (Nelson et al., 2010). These mechanistic studies call for a better understanding of the brain distribution, metabolism, and time-concentration relationships of PAS and its major metabolite, *N*-acetyl-*para*-aminosalicylic acid (AcPAS; *N*-acetyl-4-amino-2-hydroxybenzoic acid; CAS number, 50-86-2) in the targeted brain regions. It is surprising to note that the pharmacokinetic behavior of PAS, particularly with regard to its brain distribution, time profiles, and potential cerebral metabolism, remains unknown although PAS has a long history of clinical application as an antituberculosis drug. The lack of kinetic knowledge of PAS and its metabolism has hindered the understanding of the effectiveness of

This work was supported in part by the National Institutes of Health National Institute of Environmental Health Sciences [Grant R01-ES008146]; the United States Army Medical Research and Materiel Command [Contract W81XWH-05-1-0239]; and the National Major Special Project for Science and Technology Development, Ministry of Science and Technology of China [Grant 2009ZX09304-003].

Article, publication date, and citation information can be found at <http://dmd.aspetjournals.org>.

doi:10.1124/dmd.111.040915.

**ABBREVIATIONS:** PAS, 4-amino-2-hydroxybenzoic acid; AcPAS, *N*-acetyl-4-amino-2-hydroxybenzoic acid;  $AUC_{0-\infty}$ , area under the concentration-time curve from time zero to infinity;  $C_{max}$ , maximal plasma concentration after dosing; CSF, cerebrospinal fluid; HPLC, high-performance liquid chromatography; TEMED, *N,N,N',N'*-tetramethylethylenediamine;  $T_{max}$ , time to reach  $C_{max}$ .

PAS in clinics as well as the in-depth investigations on its mechanism of action.

To assist the clinical investigations of the efficacy of PAS, we have recently developed a new high-performance liquid chromatographic (HPLC) method to quantify the plasma and tissue concentrations of PAS and AcPAS (Hong et al., 2011). Our preliminary study revealed that PAS can be readily N-acetylated to form N-acetyl-PAS. After femoral artery injection, both compounds can be detected in blood and brain regions. This finding prompted us to investigate the time courses of PAS and AcPAS in plasma and brain regions where manganese is known to accumulate, whether PAS or AcPAS is more responsible for manganese chelating, and how the patterns of their brain distribution may relate to the effectiveness of PAS in reducing manganese concentrations in brain. It is understandable that a single pharmacokinetic study would not be sufficient to address all of these interesting research subjects. Thus, as an initial step toward understanding PAS treatment, we conducted this study 1) to determine pharmacokinetic parameters of PAS after intra-arterial injection of PAS so as to fill the gaps in PAS literature; 2) to determine and compare the time dependencies of PAS and AcPAS concentrations in plasma, cerebrospinal fluid (CSF), and selected brain regions after PAS administration; and 3) to determine the pharmacokinetic-pharmacodynamic relationships between PAS and AcPAS by comparing the current results with data from our earlier chelation study (Zheng et al., 2009). The results from this study will be useful for better designing PAS dosing regimens for clinical uses, future research to explore PAS actions, and more effective drug structures for therapeutic intervention in manganese-induced parkinsonian disorders.

#### Materials and Methods

**Chemicals.** Chemicals were obtained from the following sources: PAS, 5-aminosalicylic acid, 2-mercaptoethanol, phenylmethylsulfonyl fluoride, polyacrylamide, and TEMED were purchased from Sigma-Aldrich (St. Louis, MO). AcPAS was synthesized in our laboratory (Hong et al., 2011). HPLC-grade water was prepared using NANOpure Diamond Ultrapure Water Systems (Barnstead International, Dubuque, IA). All reagents were of analytical grade, HPLC grade, or the best available pharmaceutical grade.

**Animals.** Male Sprague-Dawley rats were purchased from Harlan (Indianapolis, IN) and weighed  $250 \pm 10$  g (mean  $\pm$  S.D.) at the time of the experiments. The animals were acclimatized for 1 week before experimentation in a temperature-controlled room with a 12-h light/dark cycle and were allowed free access to water and food. Before the experiment, animals fasted for 12 h, but with free access to distilled, deionized water. The study was conducted in compliance with standard animal use practices and was approved by the Institutional Animal Care and Use Committee at Purdue University.

**PAS Administration and Biological Sample Collection.** PAS was dissolved daily in sterile saline before administration. There were six groups for each time point ( $n = 6$ ). For each group, 10 rats were anesthetized with ketamine/xylazine by intraperitoneal injection, followed by PAS injection (200 mg/kg) via the femoral artery. Animals were killed at 0, 5, 15, 30, and 45 min, 1, 1.5, 2, 4, and 8 h after dosing. At each time point, CSF samples were first obtained using a 26-gauge butterfly needle (BD Biosciences, Franklin Lakes, NJ) inserted between the protuberance and the spine of the atlas and were free of blood. Blood samples were then collected from the inferior vena cava into a 2-ml heparinized syringe, and an aliquot (200  $\mu$ l) of the plasma was collected. The rat brain was perfused with saline at a flow rate of 0.8 ml/min through the left common carotid artery. After the 15-min perfusion, the brain was removed from the skull, washed with ice-cold saline, and then placed on an ice-cold filter paper on glass. The choroid plexus, striatum, hippocampus, motor cortex, cerebellum, and thalamus were dissected and homogenized using a homogenization buffer containing 20 mM Tris, pH 7.5, 5 mM EGTA, 1% Triton X-100, 0.1% SDS, 10  $\mu$ l/ml phenylmethylsulfonyl fluoride, 15 mM 2-mercaptoethanol, and a protease inhibitor cocktail (Calbiochem, San Diego, CA) in a ratio of 1:3 for tissue to buffer. The CSF, plasma, and brain homogenates were placed in Eppendorf tubes and immediately frozen at

$-80^{\circ}\text{C}$  until analysis. The samples were processed for HPLC analysis within 3 days.

**HPLC Analysis.** The concentrations of PAS and its metabolite AcPAS in plasma and selected brain regions were quantified using a well established HPLC method developed in this laboratory (Hong et al., 2011). 5-Aminosalicylic acid (CAS number, 89-57-6), a structural analog to PAS, was used as an internal standard. The plasma and tissue samples were thawed at room temperature. One volume (200  $\mu$ l) was mixed with an equal volume (200  $\mu$ l) of the internal standard working solution to achieve final internal standard concentrations of 10  $\mu$ g/ml. The samples were then mixed with an aliquot (300  $\mu$ l) of methanol, and the pH was adjusted to 1.0 by adding a small volume of 6.0 M hydrochloric acid. After vortex mixing for 1 min, the suspension was centrifuged at 12,000g for 20 min, dried under nitrogen, and reconstructed in 150  $\mu$ l of the mobile phase. An aliquot (50  $\mu$ l) of the solution was injected into the HPLC for analysis. All samples were analyzed within the same day of preparation.

A Waters 2695 XE separation module liquid chromatographic system equipped with a built-in autosampler and a Waters 2475 multi  $\lambda$  fluorescence detector was used for separation and quantification (Waters, Milford, MA). An excitation wavelength of 337 nm and an emission wavelength of 432 nm were selected for the study. Separation was accomplished using an Econosphere C18 column (5  $\mu$ m,  $250 \times 4.6$  mm) attached to a Spherisorb guard column (5  $\mu$ m,  $10 \times 4.6$  mm). The analytical and guard columns were purchased from Alltech Associates (Deerfield, IL). An isocratic mobile phase consisted of methanol and 17.5 mM potassium phosphate buffer, pH 3.5 (equal molar concentration of monobasic and dibasic potassium salts) was used for separation. Empower Version Build 1154 (Waters) was used to collect and analyze the data. Each batch included a freshly prepared standard curve (six samples between 0.05 and 500  $\mu$ g/ml) with one quality control sample for every 10 research samples. The method validation was performed according to the bioanalytical method validation guidance published by the U.S. Food and Drug Administration (Hong et al., 2011). For the protein-binding study, the calibration curve parameters, derived by the statistical analysis of independently prepared seven-point calibration curves of PAS and AcPAS in homogenization buffer, showed an excellent linearity of the assay standards. The assays have been validated for their excellent precision, sensitivity, and accuracy on the matrices. The stability study confirmed that there were no stability-related problems during the experiments or the storage of samples.

**Protein (Tissue) Binding Study.** In vitro plasma or brain protein binding experiments were performed using ultrafiltration. Stock solutions of both compounds were spiked into 1.2 ml of blank plasma samples or brain homogenates to achieve the final concentrations according to the  $C_{\text{max}}$  values obtained from the plasma or cerebral pharmacokinetic studies. Samples were allowed to equilibrate in a water-bath shaker at  $37^{\circ}\text{C}$  for 1 h. An aliquot (0.5 ml) was collected for determination of total drug concentration according to the HPLC procedure described under *HPLC Analysis*. A second aliquot (0.5 ml) of plasma or brain sample was added to a Microcon ultrafiltration system (Millipore Corporation, Billerica, MA) with a membrane molecular mass cutoff at 30 kDa. The system was centrifuged at 1500g for 15 min, and a small volume (less than 0.1 ml) of filtrate was used for HPLC analysis of free, unbound drug concentrations. The free, unbound fraction of drug was calculated as the ratio of drug concentration in the filtrate to that in plasma or brain homogenate before ultrafiltration. Nonspecific membrane binding was estimated by dissolving the tested compounds in protein-free homogenization buffer, conducting ultrafiltration without incubation under the same experimental conditions, and quantifying drug concentrations in unfiltered and filtered samples by HPLC.

**Pharmacokinetic and Statistical Analyses.** The concentration-time profiles of PAS and AcPAS in plasma, CSF, and brain tissues were analyzed by noncompartmental methods using software DAS version 2.0.1 (Mathematical Pharmacology, Professional Committee of China, Shanghai, People's Republic of China). Values of  $C_{\text{max}}$  and  $T_{\text{max}}$  were obtained directly from concentration-time profiles.

All data are presented as mean  $\pm$  S.D. Statistical analysis for comparison of two means was performed using one-way analysis of variance with post hoc comparisons by the Dunnett's tests (Kaleidagraph 3.6; Synergy Software, Reading, PA). In all cases, a probability level of  $p < 0.05$  was considered as the criterion of significance.

## Results

**Pharmacokinetics of PAS and AcPAS in Blood and CSF.** After femoral artery injection of PAS (200 mg/kg) in Sprague-Dawley rats, the concentration-time profile of PAS in plasma followed a multiexponential equation:  $C(t)_{\text{PAS}} = 5160.0e^{-1.04t} + 442.2e^{-0.02t}$  ( $R^2 = 0.999$ ).

In general, PAS was rapidly eliminated from the plasma with an initial fast phase between 0 and 1.5 h and a slow terminal phase between 1.5 and 2 h (Fig. 1A). The terminal elimination  $t_{1/2}$  of PAS was 34 min. By 4 h, PAS concentrations in plasma were nearly undetectable. In contrast, the concentration of AcPAS, a major metabolite of PAS, rose slowly, yet steadily, in plasma and reached the  $C_{\text{max}}$  at 86 min after PAS administration (Fig. 1A). The area under the curve ( $AUC_{0-\infty}$ ) of the parent PAS in plasma was approximately 3-fold greater than that of AcPAS (Table 1).

In the CSF, PAS concentrations rose rapidly and reached the  $C_{\text{max}}$  at 17 min after injection of PAS (Fig. 1B). It is noteworthy that the CSF profile of AcPAS reached the  $C_{\text{max}}$  at 44 min. The  $AUC_{0-\infty}$  of CSF PAS was approximately 7.5-fold greater than that of AcPAS in the CSF. The results suggested that PAS rapidly distributed from the blood compartment into the CSF compartment, and the metabolite AcPAS in the CSF seemed likely to result from AcPAS present in the blood and/or AcPAS formed in the brain.

**Pharmacokinetics of PAS and AcPAS in Selected Brain Regions.** After administration of PAS, the highest tissue concentrations of PAS and AcPAS were reached in the choroid plexus (Fig. 2A). The  $C_{\text{max}}$  of PAS in the choroid plexus was approximately 3.6-fold higher than that in the CSF but approximately 12- to 19-fold higher than in the other brain regions examined (Table 1). Although the  $T_{\text{max}}$  in the

choroid plexus was 29 min, the  $T_{\text{max}}$  values in the striatum (Fig. 2B), hippocampus (Fig. 2C), and motor cortex (Fig. 2D) were between 42 and 72 min, indicating a lag time for PAS to reach these brain regions; choroid plexus was the earliest and striatum the latest tissues to reach their maximums. The tissue PAS levels rapidly reached  $C_{\text{max}}$  in cerebellum (5 min) (Fig. 2E) and thalamus (15 min) (Fig. 2F) and quickly declined thereafter. It has been reported in the literature that cerebellum and thalamus are brain regions with abundant blood flow from the cerebral vasculature (Schmahmann, 2003; Rhoton, 2007).

After the administration of PAS, the metabolite AcPAS displayed distinct kinetic characteristics in brain regions. The  $t_{1/2}$  values of AcPAS in most brain regions tended to be longer than those of PAS in the same brain regions (Table 1). Except for the choroid plexus, the  $AUC_{0-\infty}$  and  $C_{\text{max}}$  values of AcPAS in most brain regions were significantly higher than those of the parent PAS (Fig. 2, B-F; Table 1). Striatum typically exhibited the greatest ratio of  $C_{\text{max(AcPAS)}}$ / $C_{\text{max(PAS)}}$ , with a value of 2.51, and hippocampus had the highest  $AUC_{\text{(AcPAS)}}$ / $AUC_{\text{(PAS)}}$  ratio, with a value of 5.07. By normalizing the brain regional  $AUC_{0-\infty}$  to the corresponding plasma  $AUC_{0-\infty}$  of PAS or AcPAS, it became evident that the tissue to plasma  $AUC_{0-\infty}$  ratios of PAS were significantly lower than those of AcPAS in all six brain regions (Fig. 3).

**Plasma Protein and Brain Tissue Binding.** The higher tissue concentrations of AcPAS compared with PAS prompted us to ask whether PAS had a higher protein binding capability than AcPAS in plasma. To test this hypothesis, we conducted protein binding experiments to determine the free, unbound PAS and AcPAS levels in plasma and six selected brain regions after ultrafiltration and adjusted for nonspecific filter membrane binding. Our data showed that a very high percentage (>90%) of the PAS molecules existed in the free, unbound state, whereas the unbound AcPAS fractions were between 80 and 87% (Table 2). PAS and AcPAS appeared to exist in plasma and brain tissues mainly in the free, unbound form. AcPAS exhibited higher plasma and tissue binding than PAS did.

**Tissue Levels of PAS/AcPAS and Their Efficacy in Manganese Chelation.** Our previous results have shown that treatment of manganese-exposed rats with PAS leads to reduced manganese concentrations in rat brains (Zheng et al., 2009). To understand whether this is due to PAS or its metabolite AcPAS, we calculated the percentage reduction in manganese concentrations in brain regions after the rats received PAS at a dose of 200 mg/kg i.p. for 3 weeks (Zheng et al., 2009) and correlated the reduction percentage with the  $AUC_{0-\infty}$  of either PAS or AcPAS in the same regions (Table 1). Linear regression analysis revealed that the percentage of manganese reduction in brain regions was better correlated with the  $AUC_{0-\infty}$  values of AcPAS ( $p < 0.05$ ) than those of PAS ( $p > 0.05$ ) (Fig. 4). It is noteworthy that the brain regions where the metabolite AcPAS was detected at the higher level (e.g., hippocampus, striatum, and thalamus) were the regions where manganese levels were reduced more effectively after PAS treatment. PAS and AcPAS may play roles in reducing tissue accumulations of manganese, AcPAS being more effective than PAS, although other mechanisms should not be excluded.

## Discussion

PAS has been used in clinics as the secondary choice for the treatment of tuberculosis since the 1950s (Mitnick et al., 2003). To our surprise, its cerebral pharmacokinetic behavior remains unknown. Thus, the study presented in this report was intended to fill the gaps with regard to the pharmacokinetics and brain distribution of PAS in a rat model. The plasma kinetics of PAS show the following characteristics. First, upon intra-arterial injection, PAS was rapidly eliminated from the blood compartment and rapidly

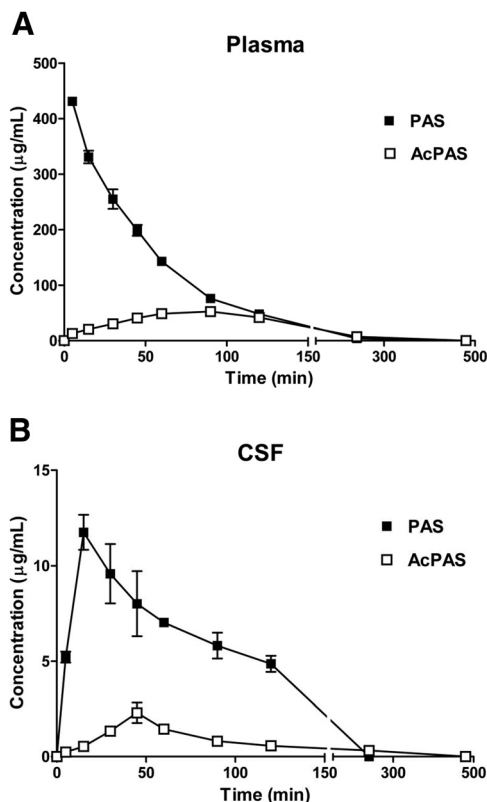


FIG. 1. Concentration-time profiles of PAS and AcPAS in body fluids. The rats received single femoral artery injections of PAS at 200 mg/kg. At the times indicated, animals ( $n = 6$ ) were anesthetized, and CSF and blood were collected for quantification of PAS and AcPAS. A, PAS and AcPAS in plasma. B, PAS and AcPAS in CSF. Data represent mean  $\pm$  S.D.

TABLE 1

Pharmacokinetic parameters of PAS and AcPAS in rat plasma, CSF, and brain regions

Data represent mean ± S.D., n = 6.

Analyte	AUC <sub>0-∞</sub> μg · min <sup>-1</sup> · g <sup>-1</sup>	C <sub>max</sub> μg/g	t <sub>1/2</sub>	T <sub>max</sub> min	MRT
Plasma					
PAS	24,914 ± 492.9	431.0 ± 7.6	34.1 ± 0.6	4.7 ± 0.5	51.1 ± 1.1
AcPAS	8336.3 ± 120.4	52.7 ± 3.2	147.2 ± 8.6	86.3 ± 15.0	205.1 ± 11.9
CSF					
PAS	1572.8 ± 112.1	11.9 ± 0.8	99.1 ± 11.3	17.2 ± 4.1	146.9 ± 15.1
AcPAS	207.8 ± 25.7	2.3 ± 0.5	75.2 ± 40.4	44.0 ± 3.1	124.9 ± 36.5
Choroid plexus					
PAS	3483.0 ± 410.6	42.8 ± 4.9	42.7 ± 8.8	29.2 ± 3.3	73.9 ± 12.3
AcPAS	2239.3 ± 183.2	30.7 ± 3.5	48.6 ± 4.6	31.3 ± 4.1	84.4 ± 3.0
Striatum					
PAS	673.1 ± 41.5	2.2 ± 0.3	174.6 ± 16.0	72.3 ± 2.0	287.8 ± 22.2
AcPAS	836.5 ± 13.1	5.4 ± 0.3	101.0 ± 9.6	53.5 ± 6.4	134.0 ± 6.3
Hippocampus					
PAS	239.8 ± 49.6	3.0 ± 0.2	77.3 ± 39.2	44.0 ± 3.1	119.0 ± 43.9
AcPAS	1215.8 ± 83.9	6.4 ± 0.3	111.8 ± 10.5	45.7 ± 5.5	173.9 ± 12.6
Motor cortex					
PAS	274.7 ± 40.2	3.2 ± 0.4	54.2 ± 30.7	42.3 ± 5.1	92.1 ± 33.3
AcPAS	619.5 ± 24.1	5.1 ± 0.4	81.6 ± 9.7	44.0 ± 3.1	128.2 ± 10.3
Cerebellum					
PAS	291.3 ± 47.8	3.6 ± 0.2	67.7 ± 15.7	4.8 ± 0.8	94.2 ± 21.9
AcPAS	1068.0 ± 29.1	3.8 ± 0.3	180.5 ± 8.1	40.8 ± 9.5	272.9 ± 9.5
Thalamus					
PAS	215.2 ± 38.0	2.6 ± 0.4	97.1 ± 38.4	15.0 ± 2.0	129.2 ± 48.2
AcPAS	933.9 ± 126.1	4.0 ± 0.4	139.5 ± 37.2	48.5 ± 5.1	216.0 ± 51.9

MRT, mean residence time.

entered the CSF, cerebellum, and thalamus. Second, among the brain tissues studied, the choroid plexus contained the highest PAS concentration, approximately 10- to 20-fold higher than other regions. Most PAS molecules were present as free, unbound PAS

in plasma, CSF, and brain tissues. Third, PAS was extensively metabolized to form AcPAS; the latter reached higher brain tissue concentrations and possessed a longer t<sub>1/2</sub> than the parent PAS did. Finally, the concentrations of PAS and its metabolite AcPAS

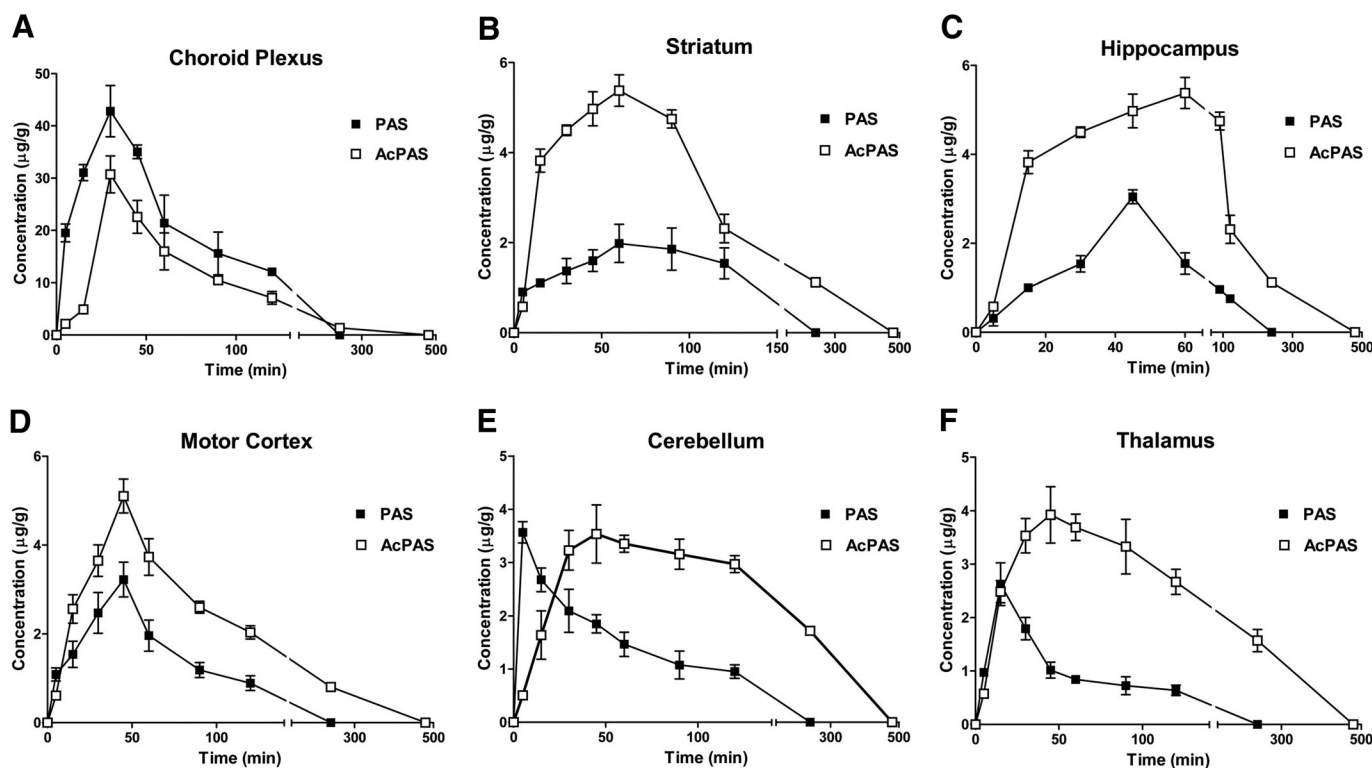


FIG. 2. Concentration-time profiles of PAS and AcPAS in selected brain regions. The rats received single femoral artery injections of at 200 mg/kg. At the times indicated, animals (n = 6) were anesthetized, and brain tissues were dissected for quantification of PAS and AcPAS. A, PAS and AcPAS in choroid plexus. B, PAS and AcPAS in striatum. C, PAS and AcPAS in hippocampus. D, PAS and AcPAS in motor cortex. E, PAS and AcPAS in cerebellum. F, PAS and AcPAS in thalamus. Data represent mean ± S.D.



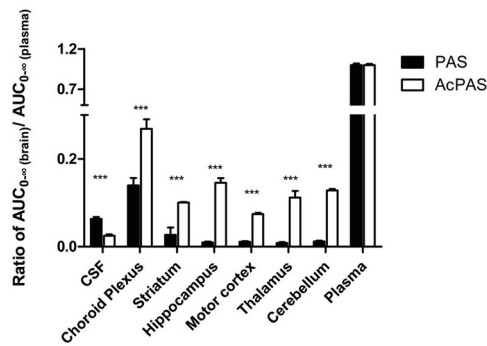


FIG. 3. Ratios of brain/CSF  $AUC_{0-\infty}$  of PAS or AcPAS versus respective plasma  $AUC_{0-\infty}$  of PAS or AcPAS. Data represent mean  $\pm$  S.D.,  $n = 6$ . \*\*\*,  $p < 0.0001$  compared between PAS and AcPAS.

appeared to be associated directly with the efficacy of PAS in reducing the tissue burden of manganese.

The finding of a fast elimination of PAS in plasma and brain tissues supports the clinical observation that high PAS doses are required to achieve effective therapeutic outcomes (Jiang et al., 2006). This observation is also consistent with our previous animal results that indicated that a high dose of PAS (200 mg/kg) acts far more effectively than low doses of PAS in reducing manganese levels in brain tissues (Zheng et al., 2009). The relatively short  $t_{1/2}$  may not allow sufficient PAS to pass across the brain barriers to achieve effective therapeutic concentrations in the brain areas in which manganese ions accumulate. Our results are also consistent with the current practice in clinics of administering PAS daily via intravenous infusions rather than administering a single-dose injection or oral dose to manganese patients (Jiang et al., 2006). Clearly, a constant high blood level of PAS achieved by intravenous infusion allows drug molecules to distribute to the targeted brain regions. It is known that manganese preferentially accumulates in the choroid plexus, striatum, and hippocampus (Roels et al., 1997; Lai et al., 1999; Zheng et al., 1999, 2009; Li et al., 2006; Reaney et al., 2006). This was also proven true by comparing the current kinetic data with our earlier chelating experiments (Zheng et al., 2009) because brain regions having high PAS and AcPAS concentrations were the regions in which PAS therapy exerted maximal reductions of manganese.

The question is whether PAS or its major metabolite AcPAS is the essential molecule in removing manganese from the brain. Recent studies suggested that the action of PAS in alleviating Parkinsonism is more likely related to its chelating abilities than its anti-inflammatory properties (Zheng et al., 2009; Nelson et al., 2010). Because PAS and AcPAS contain carboxyl and hydroxyl groups, these unique structural

TABLE 2

Brain tissue protein binding of PAS and AcPAS

Data represent mean  $\pm$  S.D.,  $n = 5$ .

Plasma/Tissues	PAS		AcPAS	
	Concentration	$F_{\text{unbound}}$	Concentration	$F_{\text{unbound}}$
	$\mu\text{g/g}$	%	$\mu\text{g/g}$	%
Plasma ( $\mu\text{g/ml}$ )	431.00	102.4 $\pm$ 3.2	52.70	80.7 $\pm$ 2.2**
Choroid plexus	42.81	91.5 $\pm$ 8.0	30.70	86.8 $\pm$ 5.0
Striatum	2.17	93.0 $\pm$ 4.0	5.44	80.3 $\pm$ 2.0*
Hippocampus	3.04	99.1 $\pm$ 4.3	6.36	85.3 $\pm$ 2.5*
Motor cortex	3.24	101.3 $\pm$ 3.0	5.10	82.0 $\pm$ 1.7**
Cerebellum	3.57	102.8 $\pm$ 5.6	3.75	81.5 $\pm$ 3.1*
Thalamus	2.63	98.5 $\pm$ 4.5	4.02	84.2 $\pm$ 2.8*

$F_{\text{unbound}}$ , fraction unbound.

\*  $p < 0.001$ .

\*\*  $p < 0.0001$  compared with PAS.

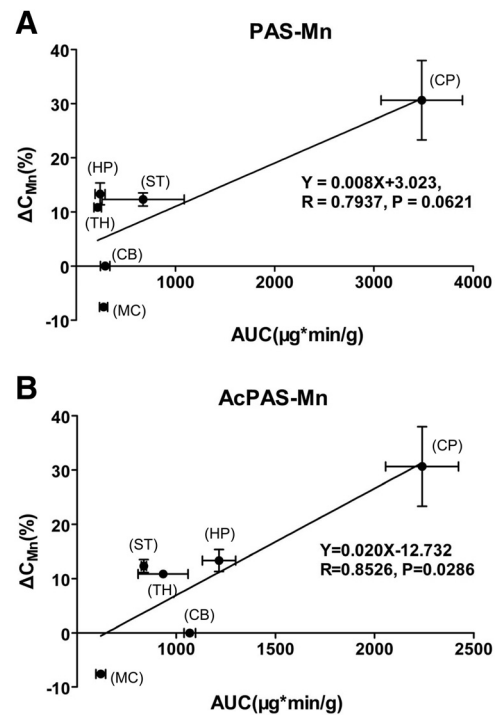


FIG. 4. Linear regression analysis of the association between brain  $AUC_{0-\infty}$  and percentage manganese reduction in brain regions (%) after PAS treatment. A, PAS  $AUC_{0-\infty}$  and percentage manganese reduction. B, AcPAS  $AUC_{0-\infty}$  and percentage manganese reduction. The percentage manganese reduction data are derived from the report by Zheng et al., 2009. CP, choroid plexus; CB, cerebellum; MC, motor cortex; HP, hippocampus; ST, striatum; TH, thalamus.

properties confer both molecules with the essential moieties to chelate manganese. From the kinetic point of view, however, the tissue  $C_{\text{max}}$  and  $AUC_{0-\infty}$  of the metabolite AcPAS were much greater than those of parent PAS. Thus, it is tempting to postulate that AcPAS may play a more important role than PAS in chelating and mobilizing manganese from the brain. This conjecture, however, requires further studies, such as the determination of in vitro dissociation constants between the two drug molecules and manganese, and the experiments in which the compounds and manganese are administered to animals, to directly compare the efficacy of the two compounds.

Our results clearly indicate that the AcPAS concentration is much higher than that of PAS in local brain regions. Several factors may contribute to the higher tissue level of AcPAS, including faster influx transport by brain barriers and/or slower efflux clearance from the brain. The lower water solubility or higher lipophilicity may allow AcPAS molecules to cross the brain barriers via passive diffusion more readily than does PAS. On the other hand, AcPAS has a stronger tissue binding affinity with brain tissue proteins. Upon reaching the brain regions in which manganese accumulates, the higher tissue binding of AcPAS may allow the AcPAS to be eliminated by brain barrier systems and spinal cord more slowly than PAS, although both PAS and AcPAS are present mainly in the free, unbound form.

The high tissue concentration of AcPAS could also be due to the conversion of PAS to AcPAS by arylamine *N*-acetyltransferase. Results from our own studies (Hong et al., 2011) and human studies by other laboratories (Dupret et al., 1994; Goodfellow et al., 2000) have established that arylamine *N*-acetyltransferase is capable of metabolizing PAS to AcPAS. The metabolism could happen in plasma and liver, and AcPAS in brain could be the result of the AcPAS in the blood diffusing into the brain. This may be the case for AcPAS in the CSF and choroid plexus because the time profiles of AcPAS in

the CSF and choroid plexus paralleled those of plasma AcPAS. However, when the time profiles of striatum, hippocampus, cortex, cerebellum, and thalamus were compared with those of AcPAS in plasma, it became clear that AcPAS in these brain regions had a rather sharp increase that is distinctly different from the pattern of the plasma AcPAS. Thus, it is reasonable to suggest that PAS may be biotransformed to AcPAS by cerebral endothelial cells that constitute the blood-brain barrier, by brain cells in the targeted area, or both. The presence of arylamine *N*-acetyltransferase has indeed been demonstrated in mouse brain regions, including the cortex and cerebellum (Sugamori et al., 2003).

Finally, the high level of AcPAS in brain tissues could also be due to an ineffective clearance of the molecules by the efflux-transport systems expressed at brain barriers (Zheng et al., 2003). For example, P-glycoprotein at the blood-brain barrier has been shown to exclude endogenous and exogenous compounds from brain parenchyma (Sun et al., 2003). It is unclear whether P-glycoprotein transports PAS or AcPAS back into the blood or has a unique preference for one molecule over the other. The low concentration of PAS in parenchyma could be due to the highly efficient clearance of PAS from the brain interstitial fluid back into the blood by efflux transporter(s). P-Glycoprotein is also expressed at the apical side of rat choroid plexus (Sun et al., 2003; Löscher and Potschka, 2005; Daoud et al., 2008). It may regulate the influx of PAS and/or AcPAS into the epithelial cells of the choroid plexuses (the blood-CSF barrier). The exact nature of the transport of these molecules by brain barrier systems is an interesting research subject for future in-depth investigations.

In summary, this pharmacokinetic study suggests that PAS has a short plasma  $t_{1/2}$  and is capable of rapidly distributing to the CSF. PAS can be metabolized to AcPAS, which has much higher tissue concentrations and possesses a longer  $t_{1/2}$  than its parent PAS. PAS and AcPAS are present in blood and tissues as mainly free, unbound molecules. The concentrations of PAS and AcPAS appeared to be associated with manganese reduction in cerebral tissues.

#### Acknowledgments

We thank Xue Fu, Yanshu Zhang, and Andrew Monnot for technical assistance during this study and Professor Gary Carlson for proofreading of the manuscript.

#### Authorship Contributions

Participated in research design: Hong, Y. Jiang, Zeng, and Zheng.

Conducted experiments: Hong and W. Jiang.

Performed data analysis: Hong, Pan, and Zheng.

Wrote or contributed to the writing of the manuscript: Hong, Zeng, and Zheng.

#### References

Aschner M, Guilarte TR, Schneider JS, and Zheng W (2007) Manganese: recent advances in understanding its transport and neurotoxicity. *Toxicol Appl Pharmacol* **221**:131–147.

Bowler RM, Gysens S, Diamond E, Nakagawa S, Drezgic M, and Roels HA (2006) Manganese exposure: neuropsychological and neurological symptoms and effects in welders. *Neurotoxicology* **27**:315–326.

Calne DB, Chu NS, Huang CC, Lu CS, and Olanow W (1994) Manganese and idiopathic parkinsonism: similarities and differences. *Neurology* **44**:1583–1586.

Cook DG, Fahn S, and Brait KA (1974) Chronic manganese intoxication. *Arch Neurol* **30**:59–64.

Crossgrove J and Zheng W (2004) Manganese toxicity upon overexposure. *NMR Biomed* **17**:544–553.

Daoud M, Tsai C, Ahdab-Barmada M, and Watchko JF (2008) ABC transporter (P-gp/ABCB1, MRP1/ABCC1, BCRP/ABCG2) expression in the developing human CNS. *Neuropediatrics* **39**:211–218.

Dupret JM, Goodfellow GH, Janezic SA, and Grant DM (1994) Structure-function studies of human arylamine *N*-acetyltransferases NAT1 and NAT2. Functional analysis of recombinant NAT1/NAT2 chimeras expressed in *Escherichia coli*. *J Biol Chem* **269**:26830–26835.

Goodfellow GH, Dupret JM, and Grant DM (2000) Identification of amino acids imparting acceptor substrate selectivity to human arylamine acetyltransferases NAT1 and NAT2. *Biochem J* **348**:159–166.

Hong L, Jiang W, Zheng W, and Zeng S (2011) HPLC analysis of para-aminosalicylic acid and its metabolite in plasma, cerebrospinal fluid and brain tissues. *J Pharm Biomed Anal* **54**:1101–1109.

Jiang YM, Mo XA, Du FQ, Fu X, Zhu XY, Gao HY, Xie JL, Liao FL, Pira E, and Zheng W (2006) Effective treatment of manganese-induced occupational Parkinsonism with p-aminosalicylic acid: a case of 17-year follow-up study. *J Occup Environ Med* **48**:644–649.

Ky SQ, Deng HS, Xie PY, and Hu W (1992) A report of two cases of chronic serious manganese poisoning treated with sodium para-aminosalicylic acid. *Br J Ind Med* **49**:66–69.

Lai JC, Minski MJ, Chan AW, Leung TK, and Lim L (1999) Manganese mineral interactions in brain. *Neurotoxicology* **20**:433–444.

Li GJ, Choi BS, Wang X, Liu J, Waalkes MP, and Zheng W (2006) Molecular mechanism of distorted iron regulation in the blood-CSF barrier and regional blood-brain barrier following in vivo subchronic manganese exposure. *Neurotoxicology* **27**:737–744.

Löscher W and Potschka H (2005) Role of drug efflux transporters in the brain for drug disposition and treatment of brain diseases. *Prog Neurobiol* **76**:22–76.

Mitnick C, Bayona J, Palacios E, Shin S, Furin J, Alcántara F, Sánchez E, Sarria M, Becerra M, Fawzi MC, et al. (2003) Community-based therapy for multidrug-resistant tuberculosis in Lima, Peru. *N Engl J Med* **348**:119–128.

Myers JE, Thompson ML, Ramushu S, Young T, Jeebhay MF, London L, Esswein E, Renton K, Spies A, Boule A, et al. (2003) The nervous system effects of occupational exposure on workers in a South African manganese smelter. *Neurotoxicology* **24**:885–894.

Nelson M, Huggins T, Licorish R, Carroll MA, and Catapano EJ (2010) Effects of p-aminosalicylic acid on the neurotoxicity of manganese on the dopaminergic innervation of the cilia of the lateral cells of the gill of the bivalve mollusc, *Crassostrea virginica*. *Comp Biochem Physiol C Toxicol Pharmacol* **151**:264–270.

Ono K, Komai K, and Yamada M (2002) Myoclonic involuntary movement associated with chronic manganese poisoning. *J Neurol Sci* **199**:93–96.

Reaney SH, Bench G, and Smith DR (2006) Brain accumulation and toxicity of Mn(II) and Mn(III) exposures. *Toxicol Sci* **93**:114–124.

Rhoton AL Jr (2007) The cerebrum. *Anatomy, Neurosurgery* **61**:37–118; discussion 119–119.

Roels H, Meiers G, Delos M, Ortega I, Lauwerys R, Buchet JP, and Lison D (1997) Influence of the route of administration and the chemical form (MnCl<sub>2</sub>, MnO<sub>2</sub>) on the absorption and cerebral distribution of manganese in rats. *Arch Toxicol* **71**:223–230.

Schmahmann JD (2003) Vascular syndromes of the thalamus. *Stroke* **34**:2264–2278.

Seaton CL, Lasman J, and Smith DR (1999) The effects of CaNa<sub>2</sub>EDTA on brain lead mobilization in rodents determined using a stable lead isotope tracer. *Toxicol Appl Pharmacol* **159**:153–160.

Shi XY (2002) One case on chronic serious manganese treated with sodium para-aminosalicylic acid [in Chinese]. *J Baotou Medical College* **18**:161–162.

Sugamori KS, Wong S, Gaedigk A, Yu V, Abramovici H, Rozmahel R, and Grant DM (2003) Generation and functional characterization of arylamine *N*-acetyltransferase Nat1/Nat2 double-knockout mice. *Mol Pharmacol* **64**:170–179.

Sun H, Dai H, Shaik N, and Elmquist WF (2003) Drug efflux transporters in the CNS. *Adv Drug Deliv Rev* **55**:83–105.

Wu P (1991) A report of one case on the diagnostic treatment with PAS-Na [in Chinese]. *Ind Health Occup Dis* **17**:163–165.

Yoon H, Kim DS, Lee GH, Kim JY, Kim DH, Kim KW, Chae SW, You WH, Lee YC, Park SJ, et al. (2009) Protective effects of sodium para-amino salicylate on manganese-induced neuronal death: the involvement of reactive oxygen species. *J Pharm Pharmacol* **61**:1563–1569.

Zheng W, Aschner M, and Ghersi-Egea JF (2003) Brain barrier systems: a new frontier in metal neurotoxicological research. *Toxicol Appl Pharmacol* **192**:1–11.

Zheng W, Jiang YM, Zhang Y, Jiang W, Wang X, and Cowan DM (2009) Chelation therapy of manganese intoxication with para-aminosalicylic acid (PAS) in Sprague-Dawley rats. *Neurotoxicology* **30**:240–248.

Zheng W, Zhao Q, Slavkovich V, Aschner M, and Graziano JH (1999) Alteration of iron homeostasis following chronic exposure to manganese in rats. *Brain Res* **833**:125–132.

Zhao DF (1995) The Clinical Observation on manganese treated with PAS-Na [in Chinese]. *J Guiyang Medical College* **20**:327–328.

---

**Address correspondence to:** Dr. Wei Zheng, School of Health Sciences, Purdue University, 550 Stadium Mall Drive, Room 1169, West Lafayette, IN 47907. E-mail: wzheng@purdue.edu

---